Effect of Type and Content of Modified Montmorillonite on the Structure and Properties of Bio-Nanocomposite Films Based on Soy Protein Isolate and Montmorillonite

P. Kumar, K.P. Sandeep, S. Alavi, V.D. Truong, and R.E. Gorga

Abstract: The nonbiodegradable and nonrenewable nature of plastic packaging has led to a renewed interest in packaging materials based on bio-nanocomposites (biopolymer matrix reinforced with nanoparticles such as layered silicates). Bio-nanocomposite films based on soy protein isolate (SPI) and modified montmorillonite (MMT) were prepared using melt extrusion. The effect of different type (Cloisite 20A and Cloisite 30B) and content (0% to 15%) of modified MMT on the structure (degree of intercalation and exfoliation) and properties (color, mechanical, dynamic mechanical, thermal stability, and water vapor permeability) of SPI-MMT bio-nanocomposite films were investigated. Extrusion of SPI and modified MMTs resulted in bio-nanocomposites with exfoliated structures at lower MMT content (5%). At higher MMT content (15%), the structure of bio-nanocomposites ranged from intercalated for Cloisite 20A to disordered intercalated for Cloisite 30B. At an MMT content of 5%, bio-nanocomposite films based on modified MMTs (Cloisite 20A and Cloisite 30B) had better mechanical (tensile strength and percent elongation at break), dynamic mechanical (glass transition temperature and storage modulus), and water barrier properties as compared to those based on natural MMT (Cloisite Na^+). Bio-nanocomposite films based on 10% Cloisite 30B had mechanical properties comparable to those of some of the plastics that are currently used in food packaging applications. However, much higher WVP values of these films as compared to those of existing plastics might limit the application of these films to packaging of high moisture foods such as fresh fruits and vegetables.

Keywords: bio-nanocomposite films, modified montmorillonite, properties, soy protein isolate, structural characterization

Introduction

The nondegradable and nonrenewable nature of plastic packaging has led to a renewed interest in packaging materials based on biopolymers derived from renewable sources. The use of biopolymer-based packaging materials can solve the waste disposal problem to a certain extent. The increased interest in biopolymer-based packaging has resulted in the development of protein-based films from soy protein, whey protein, casein, collagen, corn zein, gelatin, and wheat gluten (Cuq and others 1998). Among all the protein sources, soy proteins have attracted attention as a potential source for bio-based packaging materials because it has excellent film forming properties (Brandenburg and others 1993; Gennadios and others 1993; Park and others 2001; Zhang and others 2001; Mauri and Anon 2006; Kurose and others 2007). Soy protein isolate (SPI) is a commercial form of soy protein that contains more than 90% protein.

SPI-based packaging films cannot meet the requirements of a cost-effective film with mechanical and barrier properties similar to those of plastics. Biopolymers made from SPI alone are extremely brittle. Plasticizers such as glycerol and polyethylene glycol impart flexibility to SPI-based biopolymer films. However, the use of plasticizers leads to significant decrease in tensile strength (TS) of the films (Wang and others 1996). Soy protein-based films have been reported to have oxygen permeability (OP) similar to that of plastic films (Brandenburg and others 1993). However, they have higher water vapor permeability (WVP) as compared to plastic films due to the hydrophilic nature of proteins. Therefore, research has been geared to develop techniques to improve mechanical and water vapor barrier properties of soy protein-based packaging materials.

Recently, a new class of materials represented by bio-nanocomposites (biopolymer matrix including proteins reinforced with nanoparticles such as montmorillonite) has proven to be a promising option in improving mechanical and barrier properties of biopolymers. The bio-nanocomposites consist of a biopolymer matrix reinforced with particles (nanoparticles) having at least 1 dimension in the nanometer range (1 to 100 nm) and exhibit much improved properties due to high aspect ratio and high surface area

MS 20091163 Submitted 11/21/2009, Accepted 3/10/2010. *Authors Kumar and Sandeep are with Dept. of Food, Bioprocessing, and Nutrition Sciences and author Gorga is with Dept. of Textile Engineering, Chemistry and Science, North Carolina State Univ., Raleigh, NC 27695, U.S.A. Author Alavi is with Dept. of Grain Science and Industry, Kansas State Univ., Manhattan, KS 66506, U.S.A. Author Truong is with U.S. Dept. of Agriculture, Agricultural Research Service, South Atlantic Area, Food Science Research Unit, Raleigh, NC 27695, U.S.A. Direct inquiries to author Sandeep (E-mail: kp_sandeep@ncsu.edu).*

Paper nr FSR-09-38 of the Journal Series of the Dept. of Food, Bioprocessing, and Nutrition Sciences, North Carolina State Univ., Raleigh, NC 27695-7624, U.S.A.

doi: 10.1111/j.1750-3841.2010.01633.x

THE Society for Food Science & Technology
Journal of Food Science
A Publication of the Institute of Food Technologists

of nanoparticles (Ray and Bousmina 2005; Rhim and Ng 2007; Zhao and others 2008). The most common class of materials used as nanoparticles are layered clay minerals such as montmorillonite (MMT), hectorite, sapnotite, and laponite. These clay minerals have been proven to be very effective due to their unique structure and properties (Zeng and others 2005). MMT has very high elastic modulus (178 GPa) as compared to most biopolymers. The high value of elastic modulus enables MMT to improve the mechanical properties of biopolymers by carrying a significant portion of the applied stress (Fornes and Paul 2003).

There are 4 possible arrangements of layered clays dispersed in a polymer matrix—phase separated or immiscible (microcomposite), intercalated, exfoliated, and disordered intercalated (partially exfoliated). In an immiscible arrangement, platelets of layered clays exist as tactoids (stack of platelets) and the polymer encapsulates these tactoids. Intercalation occurs when a monolayer of extended polymer chains penetrates into the galleries (gaps between layers of clay) of the layered silicates. Intercalation results in finite expansion (2 to 3 nm) of the silicate layers. However, these silicate layers remain parallel to each other. Extensive penetration of polymer chains into the galleries of layered silicate leads to exfoliation or delamination of silicate layers. Clay platelets are separated by 10 nm or more during exfoliation. (Dennis and others 2001; Zeng and others 2005).

Bio-nanocomposites can be obtained by several methods that include *in situ* polymerization, solution exfoliation, and melt intercalation. In the *in situ* polymerization method, monomers are intercalated into layered clays and subsequently polymerized via heat, radiation, or catalyst. In solution exfoliation, layered clays are exfoliated into single platelets using a solvent and the polymer is adsorbed onto the platelets by mixing in the clay suspension. In melt intercalation, layered clays are mixed with the polymer matrix in molten state (Zeng and others 2005). A few studies on the preparation of SPI-MMT bio-nanocomposites by solution exfoliation method have been reported (Dean and Yu 2005; Rhim and others 2005; Chen and Zhang 2006). In a recent work, bio-nanocomposite films based on SPI and MMT with improved properties were prepared using melt extrusion (Kumar 2009). There was a significant improvement in mechanical (tensile strength and percent elongation at break) and dynamic mechanical properties (glass transition temperature and storage modulus), thermal stability, and water vapor permeability of the films with the addition of MMT. However, the results showed that there is a need to further improve the properties of SPI-MMT films for commercial application.

Exfoliation is the desirable arrangement for improving the properties of nanocomposites. However, exfoliation is harder to achieve during processing because layered clays such as MMT have a strong tendency to agglomerate because of their hydrophilic nature. Better exfoliation can be achieved by increasing the interlayer distance (d-spacing) between clay layers because it enables biopolymer chains to penetrate easily into the galleries of layered clays. The d-spacing of the layered silicates can be increased by ion exchange reaction of sodium ions present in natural MMT with various organic cations such as primary or quaternary amine (Li and others 2006). The influence of the type of organic modifier (primary and secondary amine) and the extent of surface coverage of clay on the structure and mechanical properties of nanocomposites based on polypropylene and MMT has been investigated by Li and others (2006). The results showed that MMT modified with quaternary amine had longer interlayer distances and resulted in nanocomposites with improved mechanical properties. The interlayer distance also increased with an increase in the surface coverage of clays with organic modifiers.

Very few studies on the properties of bio-nanocomposites based on modified MMT have been reported in literature. Lee and others (2002) prepared bio-nanocomposites based on aliphatic polyester and 2 different types of MMT (Cloisite 30B and Cloisite 10A). Bio-nanocomposites based on Cloisite 30B showed higher degree of intercalation as compared to those based on Cloisite 10A. This was attributed to strong hydrogen bonding between aliphatic polyester and hydroxyl group in the organic modifier of Cloisite 30B. Paul and others (2003) prepared bio-nanocomposites based on polylactic acid (PLA) and different types of MMT (Cloisite Na^+, Cloisite 20A, Cloisite 25A, and Cloisite 30B) using melt blending and studied the effect of MMT type and content on the structure and thermal properties of bio-nanocomposites. The results showed that improvement in thermal stability was more pronounced for Cloisite 30B as compared to other MMT types. Magalhaes and Andrade (2009) prepared bio-nanocomposites based on thermoplastic corn starch and 2 different types of MMT (natural MMT and Cloisite 30B) using melt extrusion. Scanning electron microscopy (SEM) results showed that bio-nanocomposites based on Cloisite 30B showed a higher degree of exfoliation.

The above-mentioned studies show that the type of organic modifier has an important influence on the structure and properties of bio-nanocomposites based on modified MMT. Therefore, the objective of this study was to study the effect of different type (Cloisite 20A and Cloisite 30B) and content (0% to 15%) of modified MMT on the structure (degree of intercalation and exfoliation) and properties (color, mechanical, dynamic mechanical, thermal stability, and water vapor permeability) of SPI-MMT bio-nanocomposite films.

Materials and Methods

Materials

Soy protein isolate (Supro 760) with a protein content of 92.5% (dry basis) was obtained from Protein Technologies Intl. (St. Louis, Mo., U.S.A.). Two types of modified montmorillonites (Cloisite 20A and Cloisite 30B), commercially available as a powder (2 to 13 μm), were obtained from Southern Clay Products (Austin, Tex., U.S.A.). Cloisite 20A and Cloisite 30B are MMTs modified by the addition of quaternary ammonium salts. Cloisite 20A contains dimethyl dihydrogenated tallow ammonium chloride whereas Cloisite 30B contains methyl tallow bis-2-hydroxyethyl ammonium chloride. Tallow is derived from beef and is predominantly composed of chains with 18 carbons (approximately 65% C18; approximately 30% C16; approximately 5% C14). Hydrogenated tallow is derived from tallow by hydrogenation of the double bonds (Cui and others 2008). Cloisite 20A, containing 2 tallow groups, is more hydrophobic than Cloisite 30B. The properties of modified MMTs used in this study are given in Table 1. Glycerol, used as a plasticizer, was obtained from Fisher Scientific (Pittsburg, Pa., U.S.A.). Glycerol was chosen as the plasticizer because it is nontoxic whereas other potential polyhydric alcohols such as propylene glycol and ethylene glycol are toxic and hazardous (Wang and others 1996).

Preparation of SPI-MMT nanocomposites

Process flow diagram for the preparation and characterization of soy protein isolate (SPI)-montmorillonite (MMT) bio-nanocomposite films is shown in Figure 1. The formulation consisted of SPI (70% to 85%, dry basis), glycerol (15%, dry basis),

and MMT (0% to 15%, dry basis). All 3 types of clays (Cloisite Na^+, Cloisite 20A, and Cloisite 30B) were used at 4 different levels (0%, 5%, 10%, and 15%). The ingredients were mixed and left at room temperature for 2 h for hydration. The mixture was subsequently extruded in a twin-screw co-rotating extruder (ZSK 26, Coperion Corp., Ramsey, N.J., U.S.A.). The extruder had screw diameter of 25 mm and length to diameter ratio (L/D) of 20. The extruder was operated at a screw speed of 100 rpm. The extruder had a 5 head barrel configuration. Temperatures in the 5 head barrel were maintained at 70, 90, 100, 110, and 90 °C, respectively. The extrudate was dried in an oven at 50 °C for 48 h. The dried extrudate was ground in a grinder (MicroMill, Bel-Art Products, Pequannock, N.J., U.S.A.) for further testing and film casting.

Film casting

Bio-nanocomposite powders (4%, w/v) and deionized water were mixed for 30 min at room temperature. pH of the suspension was adjusted to 9 by adding 1 M NaOH. The suspension was heated to 95 °C and held at that temperature for 20 min with continuous stirring. Subsequently, the solution was cooled to 65 °C and 25 mL of the suspension was poured in 10-cm dia petri dishes for casting nanocomposite films. The cast petri dishes were dried at ambient conditions for 48 h. The dried films were peeled off the petri dish and preconditioned before further testing.

Structural characterization of SPI-MMT films

X-ray diffraction (XRD). X-ray diffraction studies of bio-nanocomposite powders were performed with a diffraction unit (MS Philips XLF ATPS XRD 100, Omni Scientific Instruments, Biloxi, Miss., U.S.A.) operating at 35 kV and 25 mA. The radiation was generated from a Cu-Kα source with a wavelength (λ) of 0.154 nm. The diffraction data were collected from 2θ values of 2.5 to 10° with a step size of 0.01°, where θ is the angle of incidence of the X-ray beam on the sample.

Transmission electron microscopy (TEM). The structure and morphology of bio-nanocomposite powders were visualized by a transmission electron microscope (Hitachi HF2000, Hitachi High-Technologies Europe GmbH, Krefeld, Germany) operating at 200 kV. Samples of bio-nanocomposite powders were prepared by suspending the powders in methanol. The suspension was sonicated for 5 min in an ultrasonic bath (Branson 1510, Branson Ultrasonics Co., Danbury, Conn., U.S.A.). A drop of the suspension was put on a fine-mesh carbon-coated TEM support grid (C-flat^{TM}, Protochips Inc., Raleigh, N.C., U.S.A.). After drying in air, the nanocomposite powder remained attached to the grid and was viewed under the transmission electron microscope.

Scanning electron microscopy (SEM). The morphology of the fracture surface (cross-sectional surface) of the bio-nanocomposite films was visualized using a field emission scanning electron microscope (JEOL 6400F, Japan Electron Optics Ltd.,

Table 1–Properties of modified MMTs used in this study.[A]

Commercial designation	Organic modifier	Molecular weight of organic modifier (g/mol)[B]	Modifier concentration (meq/100 g of clay)	Organic content (%)[B]	Density (g/cm^3)	d-spacing (nm)
Cloisite 20A	CH_3; CH_3-N^+-HT Cl^-; HT	551.6	95	36.4	1.77	2.42
Cloisite 30B	CH_2CH_2OH; CH_3-N^+-T Cl^-; CH_2CH_2OH	404.8	90	52.4	1.98	1.85

[A]As provided by the supplier.
[B]Kim and White (2005).
HT is hydrogenated tallow and T is tallow.

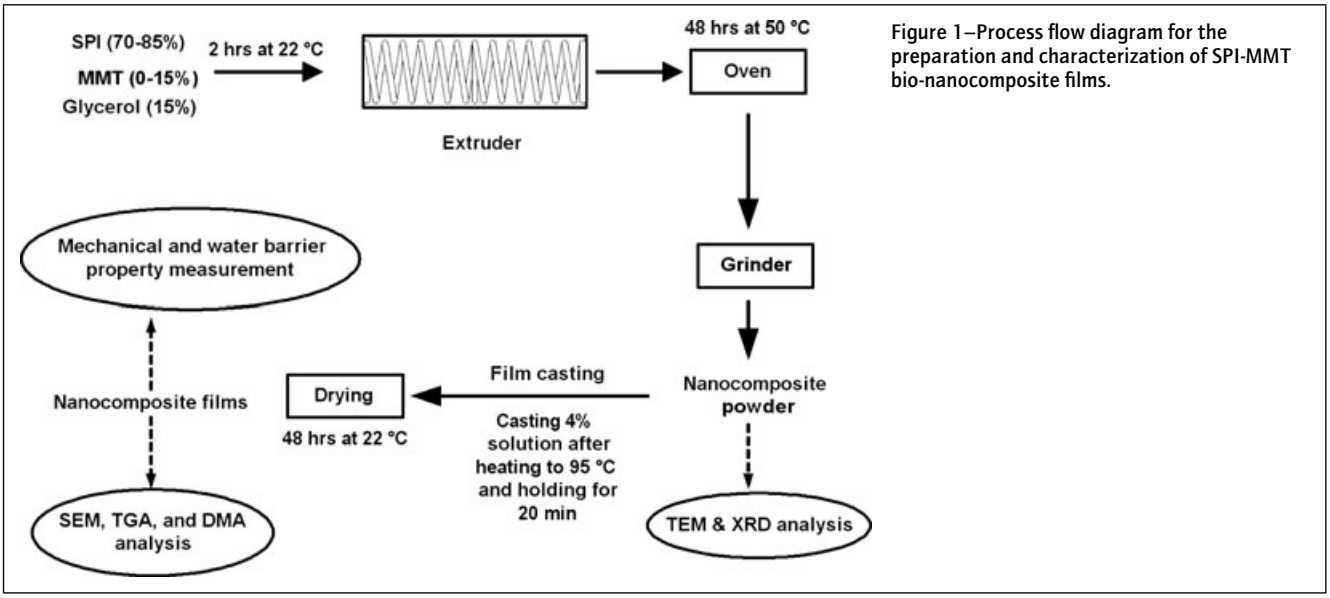

Figure 1–Process flow diagram for the preparation and characterization of SPI-MMT bio-nanocomposite films.

Tokyo, Japan) operating at 5 kV. Small pieces (0.5 × 0.5 cm) of bio-nanocomposite films were frozen in liquid nitrogen, cut using a sharp razor blade, and mounted on specimen stubs with 2-sided carbon tape. The fracture surfaces of the films were sputter-coated with a thin layer (approximately 8 to 10 nm) of gold-palladium (Au–Pd) using a sputter-coater (Hummer II, Anatech Ltd., Union City, Calif., U.S.A.). After coating, the samples were viewed under the scanning electron microscope.

Measurement of properties of SPI-MMT films

Film thickness. Thickness of the films was measured at 5 different randomly selected locations using a digital micrometer (CO 030025, Marathon Watch Co. Ltd., Ontario, Canada). The average value of the film thickness was used in determining mechanical properties, dynamic mechanical properties, and water vapor permeability.

Color. Color values of the films were measured with a Chroma Meter (CR-300, Minolta Camera Co., Osaka, Japan). Films were placed on the surface of a white standard plate (calibration plate CR-200) and the Hunter-Lab color scale (L: 0 [black] to 100 [white]; a: –80 [green] to 100 [red]; b: –80 [blue] to 70 [yellow]) was used to measure color. D_{65}, which represents daylight at noon, was used as the light source. Total color difference (ΔE), yellowness index (YI), and whiteness index (WI) were calculated as (Rhim and others 1999):

$$\Delta E = \left(\Delta L^2 + \Delta a^2 + \Delta b^2\right)^{0.5}$$
$$YI = \frac{142.86\, b}{L}$$
$$WI = 100 - \left((100 - L)^2 + \Delta a^2 + \Delta b^2\right)^{0.5} \quad (1)$$

where $\Delta L = L_{standard} - L_{sample}$; $\Delta a = a_{standard} - a_{sample}$; $\Delta b = b_{standard} - b_{sample}$. Values of L, a, and b for the standard white plate were 96.87, 0.19, and 2.00, respectively. ΔE indicates the color difference from the standard plate whereas YI and WI indicate the degree of yellowness and whiteness, respectively. Three specimens of each film sample were evaluated.

Mechanical properties. Tensile strength (TS) and percent elongation (%E) at break of the bio-nanocomposite films were determined by tensile testing using a Universal Testing Machine (model 5565, Instron, Corp., Canton, Mass., U.S.A.) equipped with a 5 kN static load cell according to the ASTM standard D882-02 (ASTM Standards 2002). The length and width of the film samples were 5 and 2.5 cm, respectively. The initial grid separation was set at 2.5 cm and the crosshead speed was 50 cm/min. Stress compared with strain curves were plotted. Tensile strength was calculated by dividing peak load by initial specimen cross-sectional area. Percent elongation at break was calculated as the percentage change in length of the specimen between the grips. Three specimens of each sample were evaluated.

Dynamic mechanical properties. The dynamic mechanical properties of bio-nanocomposite films were determined using a dynamic mechanical analyzer (Q800, TA Instruments, New Castle, Del., U.S.A.). Dynamic mechanical analysis (DMA) was performed in tension mode at a frequency of 1 Hz and an amplitude of 15 μm. The length and width of the film samples were 4 and 0.6 cm, respectively. The samples were heated from 40 to 200 °C at a heating rate of 5 °C/min. The storage modulus (E'), loss modulus (E''), and loss tangent (tan $\delta = E''/E'$) were recorded as a function of temperature. Glass transition temperature (T_g) was determined as the temperature at which tan δ attained its peak value.

Thermal stability. The thermal stability of bio-nanocomposite films was investigated using a thermogravimetric analyzer (Pyris 1 TGA, Perkin Elmer, Shelton, Conn., U.S.A.). The mass of the sample used varied from 10 to 12 mg. Thermogravimetric analysis (TGA) was carried out under airflow. The temperature of the sample was increased from room temperature to 900 °C at a heating rate of 20 °C/min. Weight loss of the sample was measured as a function of temperature. Three parameters were determined from the TGA data: the temperature at 10% weight loss, the temperature at 50% weight loss, and the yield of charred residue at 850 °C.

Water vapor permeability. WVP of the bio-nanocomposite films was determined according to ASTM E96-05 (ASTM Standards 2005). The sample film was cut into a circle of 8.75 cm dia. The sample was placed on a test dish (8.2 cm in diameter and 1.9 cm in depth) filled with 50 mL deionized water to expose the films to 100% relative humidity. The test dishes were sealed and a turntable carrying 8 test dishes was rotated uniformly to ensure that all dishes were exposed to the same average ambient conditions during the test. The setup was subjected to a temperature and relative humidity of 22 °C and 65%, respectively. The test dishes were allowed to equilibrate for 2 h before taking the initial weight. The final weight was taken after a 24-h interval. Water vapor transmission rate (WVTR) was calculated as (ASTM Standards 2005):

$$WVTR = \frac{G}{tA} \quad (2)$$

where G is the change in weight (g), t is the time (h), and A is the area of the mouth of the test dish (m^2). WVP was calculated as (ASTM standards 2005):

$$WVP = \frac{WVTR \times L}{\Delta P} \quad (3)$$

where L is the thickness of the test specimen (mm) and ΔP is the partial pressure difference of water vapor across the film. WVP of 2 specimens for each sample was calculated and reported.

Statistical analysis

All experiments were performed in duplicate. Statistical analysis was performed using Minitab statistical software (Minitab Inc., State College, Pa., U.S.A.). Data were analyzed by General Linear Model (GLM). Differences at $P < 0.05$ were considered to be significant. Pair-wise comparison of all means was performed using Tukey's multiple comparison procedure.

Results and Discussion

Effect of type and content of modified MMTs on the structure of powders/films

XRD patterns of Cloisite 20A and SPI-Cloisite 20A (0%, 5%, 10%, and 15%) bio-nanocomposite powders are shown in Figure 2. Powders of Cloisite 20A showed a diffraction peak at a 2θ angle of 3.56°. Interlayer distance (d or d-spacing) between clay layers can be estimated from Bragg's equation (Kasai and Kakudo 2005):

$$d = \frac{\lambda}{2 \sin\left(\frac{\pi\, \theta}{180}\right)} \quad (4)$$

where λ is the wavelength of X-ray beam. The d-spacing of Cloisite 20A corresponding to the diffraction peak was calculated

to be 2.48 nm. This is in close agreement with the d-spacing value of 2.42 nm provided by the supplier (Table 1). XRD patterns of Cloisite 30B and SPI-Cloisite 30B (0%, 5%, 10%, and 15%) bio-nanocomposite powders are shown in Figure 3. The d-spacing of Cloisite 30B corresponding to the diffraction peak at a 2θ angle of 5.0° was calculated to be 1.77 nm. This is in close agreement with the d-spacing value of 1.85 nm provided by the supplier (Table 1). There was no diffraction peak in the 2θ range of 2.5° to 10° for the bio-nanocomposites at all MMT contents of Cloisite 20A and Cloisite 30B. Due to the limitation of the XRD instrument, diffraction patterns below a 2θ value of 2.5° could not be observed. Absence of diffraction peaks for SPI-MMT bio-nanocomposites suggests that the layers of MMTs have a d-spacing of at least 3.53 nm (corresponding to a 2θ value of 2.5°) in all the bio-nanocomposites.

TEM images of SPI-MMT bio-nanocomposite powders with 5% and 15% contents of Cloisite 20A and Cloisite 30B are shown in Figure 4. The dark lines in the TEM images correspond to MMT platelets and the gap between 2 adjacent lines is the d-spacing. It can be seen from Figure 4A and 4C that the MMT layers are well dispersed (exfoliated) in bio-nanocomposites with MMT content of 5%. At MMT content of 15%, MMT layers are stacked together (intercalated) in bio-nanocomposites with Cloisite 20A (Figure 4B) whereas the arrangement of MMT

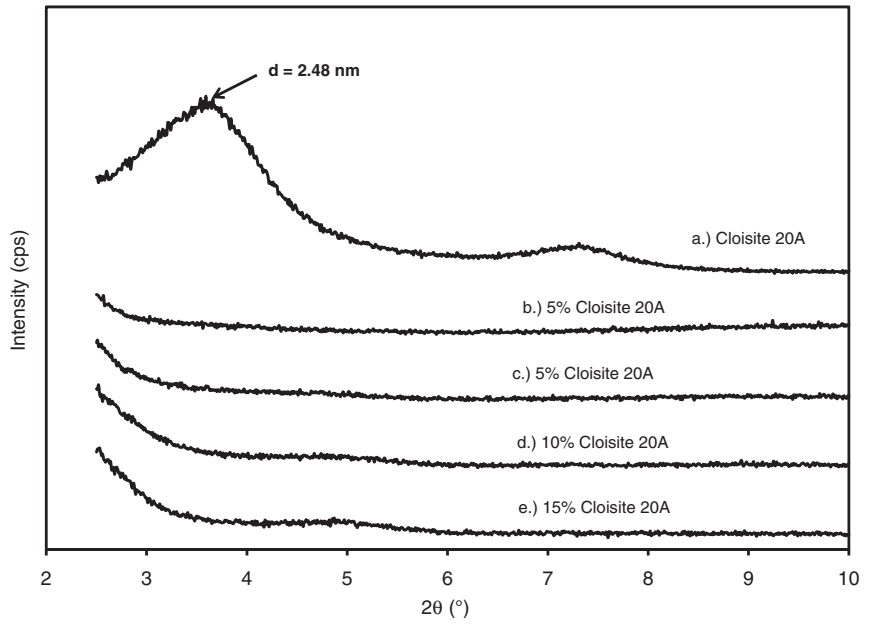

Figure 2–XRD patterns of Cloisite 20A and SPI-Cloisite 20A bio-nanocomposites with different Cloisite 20A contents.

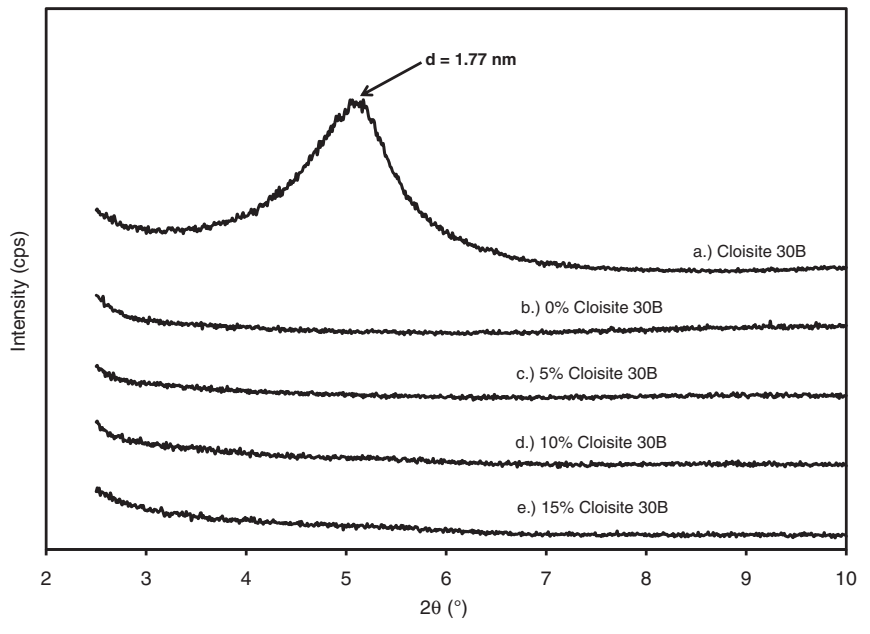

Figure 3–XRD patterns of Cloisite 30B and SPI-Cloisite 30B bio-nanocomposites with different Cloisite 30B contents.

changed from exfoliated to disordered intercalated (Figure 4D) for bio-nanocomposites with Cloisite 30B. However, d-spacing values, which ranged from 4 to 10 nm, were higher than the detection limit of XRD analysis (3.53 nm). This explains the absence of diffraction peaks for these bio-nanocomposites in the XRD analysis. Thus, it can be concluded that XRD by itself is insufficient to characterize the structure of nanocomposites for intercalated and disordered intercalated arrangements. Therefore, XRD studies should always be complemented with microscopy techniques such as TEM or SEM.

SEM images of the fracture surface (cross-sectional surface) of SPI-MMT bio-nanocomposite films with 5% and 15% contents of Cloisite 20A and Cloisite 30B are shown in Figure 5. The white strands in the SEM images correspond to MMT platelets. At an MMT content of 5%, MMT platelets were well dispersed in the bio-nanocomposite films, suggesting exfoliation of MMT in the films (Figure 5A and 5C). The fracture surface of the films with both Cloisite 20A and Cloisite 30B became rougher as the MMT content increased to 15% (Figure 5B and 5D). This can be attributed to the formation of intercalated and disordered intercalated arrangements at higher MMT content. In agreement with the TEM results of intercalated structures, larger aggregates of Cloisite 20A were found in bio-nanocomposite films with MMT content of 15% (Figure 5D).

Based on the XRD, TEM, and SEM results, it can be concluded that extrusion of SPI and modified MMTs resulted in bio-nanocomposites with exfoliated structures at lower MMT content (5%). At higher MMT content (15%), the structure of bio-nanocomposites ranged from intercalated for Cloisite 20A to disordered intercalated for Cloisite 30B.

Effect of type and content of modified MMTs on the properties of films

Hunter color values (L, a, and b) of films based on SPI and modified MMTs are shown in Table 2. SPI films without modified MMTs were translucent and yellow with L, a, and b values of 81.42, 3.61, and 44.14, respectively. Changes in color can be better described using color functions such as total color difference (ΔE), whiteness index (WI), and yellowness index (YI). There was a significant ($P < 0.05$) increase in WI of the films with the addition of 5% of modified MMTs. Further addition of modified MMTs had insignificant effect on WI. In contrast, there was a significant ($P < 0.05$) decrease in YI of the films with the addition of 5% of modified MMTs. Further addition of modified MMTs had insignificant effect on YI. It can be concluded from these results that the SPI-MMT films were lighter (higher WI) and less yellow (lower YI) as compared to those of SPI films.

The effect of type and content of modified MMTs on tensile strength of SPI-MMT films is shown in Table 3. Analysis of variance using the GLM showed that the effects of clay type, clay content, and interaction between clay type and content on TS were significant ($P < 0.05$). Tensile strength of SPI films was 2.26 ± 0.48 MPa. The values of TS for bio-nanocomposite films with 5% of Cloisite 20A and Cloisite 30B were 12.40 ± 0.65 and 15.11 ± 0.86 MPa, respectively. Kumar (2009) reported a TS value of 6.28 ± 0.88 MPa for bio-nanocomposite films based on SPI and 5% natural MMT (Cloisite Na^+). The density of natural MMT is 2.86 g/cm^3 whereas the density values of Cloisite 20A and Cloisite 30B are 1.77 and 1.98 g/cm^3. At the same MMT content, Cloisite 20A and Cloisite 30B have higher volume fractions in the bio-nanocomposites as compared to that of natural MMT. It has been

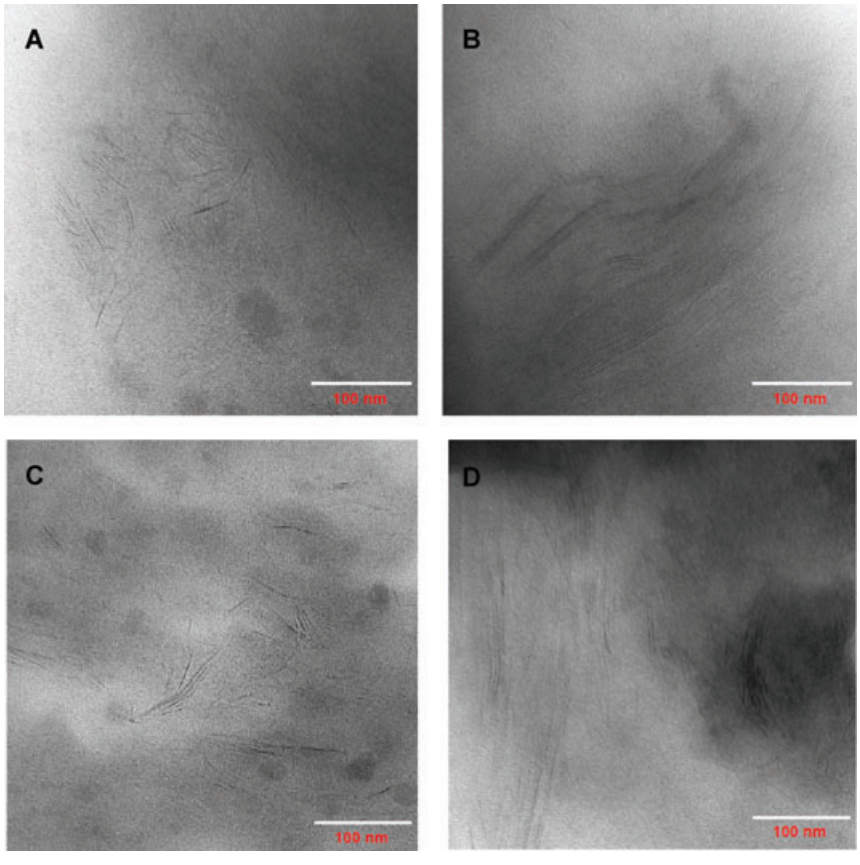

Figure 4–TEM images of bio-nanocomposites with (A) 5% Cloisite 20A, (B) 15% Cloisite 20A, (C) 5% Cloisite 30B, and (D) 15% Cloisite 30B.

reported that the improvement in properties of nanocomposites is proportional to the volume fraction of nanoparticles (Fornes and Paul 2003). Modified MMTs also have longer d-spacing values as compared to that of natural MMT. This enables better interaction of SPI with modified MMT because biopolymer chains of soy proteins can penetrate easily into the galleries of modified MMTs. Thus, the higher TS values for modified MMTs might be attributed to higher volume fraction at the same MMT content and better interaction of SPI with modified MMTs.

As MMT content increased to 10%, TS of Cloisite 20A films increased and then TS of the films decreased above 10%. Fornes and Paul (2003) reported that intercalation of layered clays in nanocomposites reduces their reinforcing efficiency due to decrease in aspect ratio and effective modulus of clays. Bio-nanocomposites with Cloisite 20A had intercalated structures at 15%. This can explain the decrease in TS of films of Cloisite 20A at a content of 15%. TS of Cloisite 30B films increased continuously as MMT content increased. However, there was only a slight increase in TS above 5% which is due to disordered intercalated structures in bio-nanocomposites with Cloisite 30B at higher MMT contents.

The effect of type and content of modified MMTs on percent elongation (%*E*) at break of SPI-MMT films is shown in Table 4.

Table 2–Effect of type and content of modified MMTs on Hunter color values (*L*, *a*, and *b*) of SPI-MMT films.[A]

Films	*L*	*a*	*b*
SPI	81.42 ± 0.99^{a}	3.61 ± 0.83^{a}	44.14 ± 2.22^{a}
SPI-5% Cloisite 20A	90.83 ± 0.04^{b}	-0.09 ± 0.02^{b}	16.42 ± 0.14^{b}
SPI-10% Cloisite 20A	88.90 ± 0.49^{b}	0.11 ± 0.02^{b}	18.07 ± 0.09^{b}
SPI-15% Cloisite 20A	88.29 ± 0.76^{b}	0.42 ± 0.05^{b}	17.29 ± 0.44^{b}
SPI-5% Cloisite 30B	86.44 ± 0.40^{c}	1.16 ± 0.05^{b}	23.77 ± 0.50^{c}
SPI-10% Cloisite 30B	87.23 ± 0.28^{c}	0.56 ± 0.06^{b}	21.99 ± 0.42^{c}
SPI-15% Cloisite 30B	88.43 ± 0.34^{c}	0.57 ± 0.11^{b}	19.89 ± 0.15^{c}

[A]Values are mean of 2 replicates ± standard deviation. Means in the same column followed by the same letter are not significantly different ($P > 0.05$).

Table 3–Effect of type and content of modified MMTs on tensile strength (TS) of SPI-MMT films.[A]

	TS (MPa)	
MMT content	Cloisite 20A	Cloisite 30B
0% MMT	2.26 ± 0.48^{a}	2.26 ± 0.48^{a}
5% MMT	12.40 ± 0.65^{b}	15.11 ± 0.86^{d}
10% MMT	14.15 ± 0.33^{c}	16.19 ± 0.75^{e}
15% MMT	13.66 ± 0.28^{c}	18.64 ± 0.23^{e}

[A]Values are mean of 2 replicates ± standard deviation. Means in the same row and column followed by the same letter are not significantly different ($P > 0.05$).

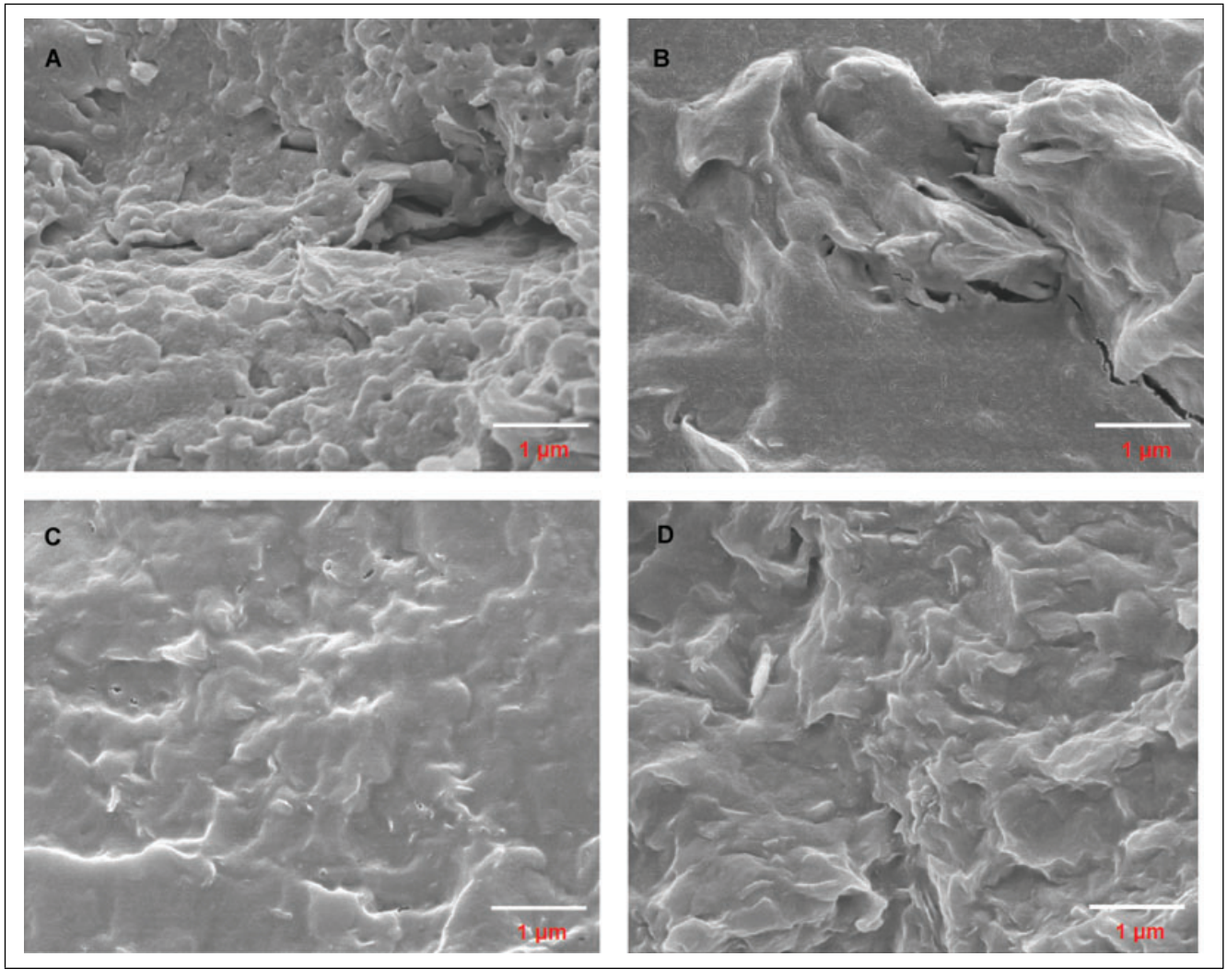

Figure 5–SEM images of bio-nanocomposite films with (A) 5% Cloisite 20A, (B) 15% Cloisite 20A, (C) 5% Cloisite 30B, and (D) 15% Cloisite 30B.

Analysis of variance using the GLM showed that the effects of clay type, clay content, and interaction between clay type and content on %*E* were significant ($P < 0.05$). Percent elongation at break of SPI films was 11.85 ± 0.39. The values of %*E* for bio-nanocomposite films with 5% of Cloisite 20A and Cloisite 30B were 42.80 ± 0.57 and 81.60 ± 2.83, respectively. As MMT content increased to 10%, %*E* of Cloisite 20A and Cloisite 30B films increased and then %*E* of the films decreased above 10%. This is attributed to the restricted motion of soy protein molecules in bio-nanocomposite films due to incorporation of MMT and interaction of SPI with MMT.

TS values of films containing 10% of both modified MMTs are comparable to those of low-density polyethylene (LDPE) and polyvinylidene chloride (PVDC), which are currently used in food packaging applications (8.2 to 31.4 MPa for LDPE and 19.3 to 34.5 MPa for PVDC). However, %*E* values for these plastic films range from 100% to 900% (Selke 1997). Maximum %*E* value obtained for SPI-MMT films was 103.6% which was obtained with Cloisite 10% 30B. This shows the potential of films based on SPI and Cloisite 30B to be used in flexible food packaging to replace some of the existing plastics such as LDPE and PVDC.

The effect of temperature on tan δ of bio-nanocomposite films based on SPI and modified MMTs at MMT contents of 0%, 5%, and 15% is shown in Figure 6. Glass transition temperature (T_g) was determined from the peak in tan δ curve. Analysis of variance using the GLM showed that the effects of clay type, clay content, and interaction between clay type and content on T_g were significant ($P < 0.05$). SPI films had a T_g of 119.7 ± 1.9 °C which is in the range of T_g (111.9 to 150 °C) of SPI films as reported by Ogale and others (2000). The values of T_g for bio-nanocomposite films with 5% of Cloisite 20A and Cloisite 30B were 154.7 ± 0.8 and 148.1 ± 0.8 °C respectively. Kumar (2009) reported a T_g value of 142.8 ± 2.1 °C for bio-nanocomposite films based on SPI and 5% natural MMT (Cloisite Na^+). It can be seen from Figure 6 that there was a slight increase in T_g as MMT content increased from 5% to 15%. However, the magnitude of the peak value of tan δ decreased as MMT content increased from 5% to 15%. The magnitude of tan δ peak is an indication of the motion of polymer chains in amorphous phase (Yu and others 2004). The reduced magnitude of tan δ peak at higher MMT contents can be attributed to restricted motion of biopolymer chains of SPI due to the interaction of SPI with MMT.

Table 4–Effect of type and content of modified MMTs on percent elongation of break (%E) of SPI-MMT films.[A]

	%E	
MMT content	**Cloisite 20A**	**Cloisite 30B**
0% MMT	11.85 ± 0.39[a]	11.85 ± 0.39[a]
5% MMT	42.80 ± 0.57[b]	81.60 ± 2.83[e]
10% MMT	71.00 ± 3.68[c]	103.60 ± 4.53[f]
15% MMT	22.80 ± 1.70[d]	54.80 ± 2.26[g]

[A]Values are mean of 2 replicates ± standard deviation. Means in the same row and column followed by the same letter are not significantly different ($P > 0.05$).

The effect of temperature on storage modulus (E') of bio-nanocomposite films based on SPI and modified MMTs at MMT contents of 0%, 5%, and 15% is shown in Figure 7. Over the entire temperature range, E' of SPI-MMT films was significantly ($P < 0.05$) higher than that of SPI films. Storage modulus of SPI films at 40 °C was 337 ± 31 MPa. The values of storage modulus for bio-nanocomposite films with 5% Cloisite 20A and Cloisite 30B were 1164 ± 37 and 870 ± 53 MPa, respectively. Kumar (2009) reported a storage modulus value of 529 ±m 24 MPa for bio-nanocomposite films based on SPI and 5% natural MMT (Cloisite Na^+). In agreement with the tensile strength results, the higher E' values for modified MMTs are attributed to higher volume fraction at the same MMT content and better interaction of SPI with modified MMTs.

TGA curves of bio-nanocomposite films based on SPI and modified MMTs at MMT contents of 0%, 5%, and 15% are shown in Figure 8. It can be seen from Figure 8 that there are 3 steps of thermal degradation of the films in the temperature range of 100 to 900 °C. The temperature range for the 1st step of thermal degradation is 100 to 150 °C. This corresponds to the loss of water from the films. The temperature range for the 2nd step of thermal degradation is 300 to 400 °C. This corresponds to the decomposition of soy protein, decomposition of organic modifiers

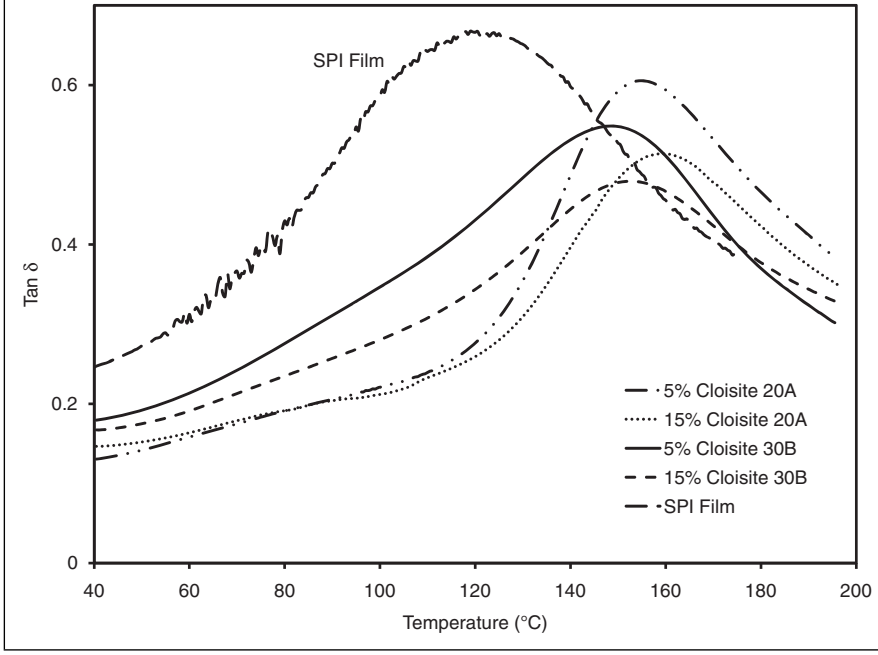

Figure 6–Effect of temperature on tan δ of bio-nanocomposite films based on SPI and modified MMTs at different MMT contents.

of modified MMT, and loss of glycerol from the films. The 3rd step of thermal degradation is in the temperature range of 500 to 750 °C. This might be due to oxidation of partially decomposed soy protein and organic modifiers under airflow. Similar results for different types of bio-nanocomposite films have been reported (Tunc and others 2007).

The temperature at 50% weight loss (during TGA) for SPI films was 355.5 ± 2.2 °C. The temperatures at 50% weight loss for bio-nanocomposite films with 5% of Cloisite 20A and Cloisite 30B were 367.7 ± 1.7 °C and 378.6 ± 2.3 °C, respectively. These temperatures are comparable to the temperature at 50% weight loss of 377.3 ± 2.6 °C for bio-nanocomposite films based on SPI and 5% natural MMT (Cloisite Na^+) as reported by Kumar (2009). As the MMT content increased, the bio-nanocomposite films exhibited a significant delay in weight loss at temperatures greater than 500 °C. The yield of charred residue at 850 °C for SPI films was 4.2 ± 0.3%. The yields of charred residue at 850 °C for bio-nanocomposite films with 15% of Cloisite 20A and Cloisite 30B were 10.9 ± 0.6% and 11.2 ± 0.4%, respectively. These yields of charred residue for modified MMTs are much lower than that (20.5 ± 0.4%) of bio-nanocomposite films based on SPI and 15% natural MMT (Cloisite Na^+) as reported by Kumar (2009). This reduction in yields of charred residue is attributed to the thermal decomposition of organic modifier of modified MMTs. Cloisite 20A and Cloisite 30B contain 36.4% and 52.4% of organic modifiers, respectively (Table 1). Cervantes-Uc and

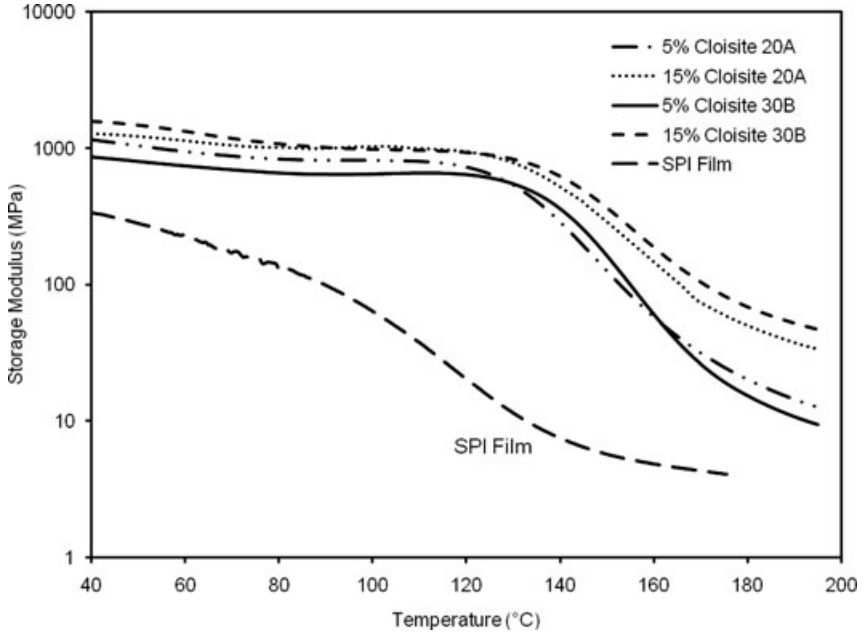

Figure 7–Effect of temperature on storage modulus of bio-nanocomposite films based on SPI and modified MMTs at different MMT contents.

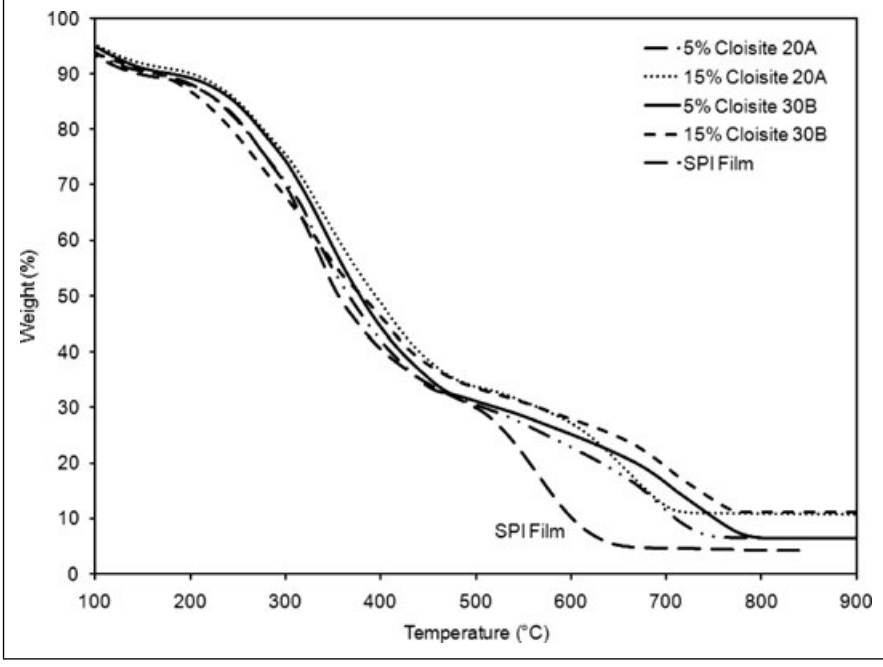

Figure 8–TGA curves of bio-nanocomposite films based on SPI and modified MMTs at different MMT contents under airflow.

Table 5–Effect of type and content of modified MMTs on water vapor permeability (WVP) of SPI-MMT films.[A]

	WVP (g·mm/m^2/h/kPa)	
MMT content	**Cloisite 20A**	**Cloisite 30B**
0% MMT	3.80 ± 0.11[a]	3.80 ± 0.11[a]
5% MMT	2.63 ± 0.03[b]	3.09 ± 0.05[e]
10% MMT	2.16 ± 0.10[c]	2.67 ± 0.08[f]
15% MMT	2.05 ± 0.11[d]	2.33 ± 0.09[g]

[A]Values are mean of 2 replicates ± standard deviation. Means in the same row and column followed by the same letter are not significantly different ($P > 0.05$).

others (2007) reported that the onset temperatures of thermal degradation for Cloisite 20A and Cloisite 30B are198 and 174 °C, respectively. This was attributed to the thermal decomposition of organic modifiers of the modified MMTs. In another study, Kim and White (2005) reported that Cloisite 20A and Cloisite 30B yield 68% and 72% of solid residues at 800 °C whereas the solid residue at 800 °C corresponding to natural MMT (Cloisite Na^+) was 88%.

The effect of type and content of modified MMTs on WVP of SPI-MMT films is shown in Table 5. Higher WVP is one of the major limitations in using protein-based films as food packaging materials. Therefore, reduction in WVP is desirable for potential applications in food packaging. Analysis of variance using the GLM showed that the effects of clay type, clay content, and interaction between clay type and content on WVP were significant ($P < 0.05$). SPI films had a WVP of 3.80 ± 0.11 g-mm/m^2/h/kPa which is comparable to the WVP (1.62 to 6.42 g-mm/m^2/h/kPa of soy protein-based films as reported in literature (Krochta 2002). The values of WVP for films with 5% Cloisite 20A and Cloisite 30B reduced by 30.8% and 18.7%, respectively. Kumar (2009) reported a reduction of 22.1% for bio-nanocomposite films based on SPI and 5% natural MMT (Cloisite Na^+). The reduction in WVP by MMT has been attributed to the creation of a tortuous pathway for water vapor to diffuse out of the bio-nanocomposite matrix. This increases the effective path length for diffusion of water vapor molecules, thus reducing WVP (Zeng and others 2005). At 5% MMT content, greater reduction in WVP associated with Cloisite 20A is attributed to the hydrophobic nature of Cloisite 20A. For Cloisite 20A, there was a slight decrease in WVP as the MMT content increased from 10% to 15%. This can be explained by the formation of intercalated structures in bio-nanocomposites based on Cloisite 20A at higher MMT content (15%) as observed in TEM and SEM results. As the MMT content increased from 0% to 15%, WVP for films containing Cloisite 20A and Cloisite 30B reduced by 46.1% and 38.7%, respectively. However, the WVP values for SPI-MMT films are still much higher as compared to those (0.001 g-mm/m^2/h/kPa for LDPE and 0.01 g-mm/m^2/h/kPa for PVDC) of LDPE and PVDC that are currently used in food packaging applications (Krochta 2003; Lange and Wyser 2003). This might limit the application of these bio-nanocomposite films to packaging of high moisture foods such as fresh fruits and vegetables.

Conclusions

The focus of this study was to achieve better exfoliation by preparing bio-nanocomposite films based on soy protein isolate (SPI) and modified montmorillonite (MMT) using melt extrusion. Better exfoliation is desirable for improving the properties of bio-nanocomposite films. The arrangement of MMT in the bio-nanocomposite matrix ranged from exfoliated to intercalated depending on the type and content of modified MMT. Bio-nanocomposite films based on modified MMTs were lighter (higher WI) and less yellow (lower YI) as compared to those of SPI films. At an MMT content of 5%, bio-nanocomposite films based on modified MMTs (Cloisite 20A and Cloisite 30B) had better mechanical (tensile strength and percent elongation at break), dynamic mechanical (glass transition temperature and storage modulus), and water barrier properties as compared to those based on natural MMT (Cloisite Na^+). However, films based on modified MMTs were thermally less stable at temperatures higher than 500 °C as compared to films based on natural MMT. Bio-nanocomposite films based on 10% Cloisite 30B had mechanical properties comparable to those of LDPE and PVDC which are currently used in food packaging applications. Thus, this study shows the potential of films based on SPI and Cloisite 30B to be used in flexible food packaging to replace some of the existing plastics such as LDPE and PVDC. However, much higher WVP values of these films as compared to those of LDPE and PVDC might limit the application of these bio-nanocomposite films to packaging of high moisture foods such as fresh fruits and vegetables. Some of the other challenges associated with commercial application of these bio-nanocomposite films include higher cost of ingredients and complexity associated with the approval of these bio-nanocomposite films as food contact materials.

Acknowledgments

Support for this study from USDA-NRICGP grant nr 2008-01503 is gratefully acknowledged. We would also like to thank Birgit Anderson, Gail Liston, Roberto Garcia, Chuck Mooney, Jonathan Pierce, and Sharon Ramsey for their assistance in conducting the experiments.

References

ASTM Standards. 2002. D882–02. Standard test method for tensile properties of thin plastic sheeting. Philadelphia, Pa.: ASTM Int.
ASTM Standards. 2005. E96–05. Standard test methods for water vapor transmission of materials. Philadelphia, Pa.: ASTM Int.
Brandenburg AH, Weller CL, Testin RF. 1993. Edible films and coatings from soy protein. J Food Sci 58:1086–9.
Cervantes-Uc JM, Cauich-Rodriguez JV, Vazquez-Torres H, Garfias-Mesias LF, Paul DR. 2007. Thermal degradation of commercially available organoclays studied by TGA-FTIR. Thermochim Acta 457:92–102.
Chen P, Zhang L. 2006. Interaction and properties of highly exfoliated soy protein/montmorillonite nanocomposites. Biomacromolecules 7:1700–6.
Cui L, Khramov DM, Bielawski CW, Hunter DL, Yoon PJ, Paul DR. 2008. Effect of organoclay purity and degradation on nanocomposite performance, part 1: surfactant degradation. Polymer 49:3751–61.
Cuq B, Gontard N, Guilbert S. 1998. Proteins as agricultural polymers for packaging production. Cereal Chem 75(1):1–9.
Dean K, Yu L. 2005. Biodegradable protein-nanoparticles composites. In: Smith R, editor. Biodegradable polymers for industrial applications. Cambridge, U.K.: Woodhead Publishing Ltd. p 289–312.
Dennis HR, Hunter DL, Chang D, Kim S, White JL, Cho JW, Paul DR. 2001. Effect of melt processing conditions on the extent of exfoliation in organoclay-based nanocomposites. Polymer 42:9513–22.
Fornes TD, Paul DR. 2003. Modeling properties of nylon 6/clay nanocomposites using composite theories. Polymer 44:4993–5013.
Gennadios A, Brandenburg AH, Weller CL, Testin RF. 1993. Effect of pH on properties of wheat gluten and soy protein isolate films. J Agric Food Chem 41:1835–9.
Kasai K, Kakudo M. 2005. X-ray diffraction by macromolecules. New York: Springer. 504 p.
Kim Y, White JL. 2005. Formation of polymer nanocomposites with various organoclays. J Appl Polym Sci 96:1888–96.
Krochta JM. 2002. Proteins as raw materials for films and coatings: definitions, current status, and opportunities. In: Gennadios A, editor. Protein-based films and coatings. Boca Raton, Fla.: CRC press. p 1–41.
Krochta JM. 2003. Package permeability. In: Heldman DR, editor. Encyclopedia of agricultural, food, and biological engineering. New York: Marcel Dekker, Inc. p 720–6.
Kumar P. 2009. Development of bio-nanocomposite films with enhanced mechanical and barrier properties using extrusion processing [PhD diss.]. Raleigh, N.C.: North Carolina State Univ. 282 p. Available from: http://www.lib.ncsu.edu/theses/available/etd-11032009–192332/unrestricted/etd.pdf. Accessed Feb 21, 2010.
Kurose T, Urman K, Otaigbe JU, Lochhead RY, Thames SF. 2007. Effect of uniaxial drawing of soy protein isolate biopolymer films on structure and mechanical properties. Polym Engr Sci 47(4):374–80.

Lange Y, Wyser Y. 2003. Recent innovations in barrier technologies for plastic ackaging—a review. Packag Technol Sci 16:149–58.
Lee SR, Park HM, Lim H, Kang T, Li X, Cho WJ, Ha CS. 2002. Microstructure, tensile properties, and biodegradability of aliphatic polyester/clay nanocomposites. Polymer 43:2495–500.
Li J, Ton-That MT, Tsai SJ. 2006. PP-based nanocomposites with various intercalant types and intercalant coverages. Polym Engr Sci 46(8):1060–8.
Magalhaes NF, Andrade CT. 2009. Thermoplastic corn starch/clay hybrids: effects of clay type and content on physical properties. Carbohyd Polym 75:712–8.
Mauri AN, Anon MC. 2006. Effect of solution pH on solubility and some structural properties of soybean protein isolate films. J Sci Food Agric 86:1064–72.
Ogale AA, Cunningham P, Dawson PL, Acton JC. 2000. Viscoelastic, thermal, microstructural characterization of soy protein isolate films. J Food Sci 65(4):672–9.
Park SK, Rhee CO, Bae DH, Hettiarachchy NS. 2001. Mechanical properties and water vapor permeability of soy protein films affected by calcium salts and glucono-δ-lactone. J Agric Food Chem 49:2308–12.
Paul MA, Alexandre M, Degee P, Henrist C, Rulmont A, Dubois P. 2003. New nanocomposite materials based on plasticized poly(L-lactide) and organo-modified montmorillonites: thermal and morphological study. Polymer 44:443–50.
Ray SS, Bousmina M. 2005. Biodegradable polymers and their layered silicate nanocomposites: in greening the 21st century materials world. Prog Mater Sci 50:962–1079.
Rhim JW, Ng PKW. 2007. Natural biopolymer-based nanocomposite films for packaging applications. Crit Rev Food Sci Nutr 47(4):411–33.
Rhim JW, Wu Y, Weller CL, Schnepf M. 1999. Physical characteristics of a composite films of soy protein isolate and propyleneglycol alginate. J Food Sci 64(1):149–52.
Rhim JW, Lee JH, Kwak HS. 2005. Mechanical and barrier properties of soy protein and clay mineral composite films. Food Sci Biotechnol 14:112–6.
Selke SEM. 1997. Understanding plastics packaging technology. New York: Hanser Publication. 206 p.
Tunc S, Angellier H, Cahyana Y, Chalier P, Gontard N, Gastaldi E. 2007. Functional properties of wheat gluten/montmorillonite nanocomposite films processed by casting. J Memb Sci 289:159–68.
Wang S, Sue HJ, Jane J. 1996. Effects of polyhydric alcohols on the mechanical properties of soy protein plastics. J Macromol Sci A 33(5):557–69.
Yu ZZ, Yan C, Yang M, Mai, YW. 2004. Mechanical and dynamic mechanical properties of nylon 66/montmorillonite nanocomposites fabricated by melt compounding. Polym Int 53:1093–8.
Zeng QH, Yu AB, Lu GQ, Paul DR. 2005. Clay-based polymer nanocomposites: research and commercial development. J Nanosci Nanotechnol 5:1574–92.
Zhang J, Mungara P, Jane J. 2001. Mechanical and thermal properties of extruded soy protein sheets. Polymers 42:2569–78.
Zhao R, Torley P, Halley PJ. 2008. Emerging biodegradable materials: starch- and protein-based bio-nanocomposites. J Mater Sci 43:3058–71.